

The Role of Dopamine in Temporal Uncertainty

Alessandro Tomassini¹, Diane Ruge¹, Joseph M. Galea^{1,2},
William Penny¹, and Sven Bestmann¹

Abstract

■ The temporal preparation of motor responses to external events (temporal preparation) relies on internal representations of the accumulated elapsed time (temporal representations) before an event occurs and on estimates about its most likely time of occurrence (temporal expectations). The precision (inverse of uncertainty) of temporal preparation, however, is limited by two sources of uncertainty. One is intrinsic to the nervous system and scales with the length of elapsed time such that temporal representations are least precise for longest time durations. The other is external and arises from temporal variability of events in the outside world. The precision of temporal expectations thus decreases if events become more variable in time. It has long been recognized that the processing of time durations within the range of hundreds of milliseconds (interval timing) strongly depends on dopaminergic (DA) transmission. The role of DA for the precision of temporal preparation in

humans, however, remains unclear. This study therefore directly assesses the role of DA in the precision of temporal preparation of motor responses in healthy humans. In a placebo-controlled double-blind design using a selective D2-receptor antagonist (sulpiride) and D1/D2 receptor antagonist (haloperidol), participants performed a variable foreperiod reaching task, under different conditions of internal and external temporal uncertainty. DA blockade produced a striking impairment in the ability of extracting temporal expectations across trials and on the precision of temporal representations within a trial. Large Weber fractions for interval timing, estimated by fitting subjective hazard functions, confirmed that this effect was driven by an increased uncertainty in the way participants were experiencing time. This provides novel evidence that DA regulates the precision with which we process time when preparing for an action. ■

INTRODUCTION

The ability to anticipate the likely time of occurrence of events (Coull & Nobre, 1998) enables temporally precise preparation of motor responses (temporal preparation from here on). Accurate temporal preparation requires the internal representation of the accumulated elapsed time before an event occurs (temporal representation; Niemi & Näätänen, 1981). The speed of motor responses thus depends on how well our internal representation of time matches the time of stimulus appearance, that is, how precise our temporal representations are. Moreover, temporal preparation requires estimates about the most likely time of occurrence of an event, given past experience (temporal expectation; Janssen & Shadlen, 2005). Our responses are thus faster when these estimates are accurate (Niemi & Näätänen, 1981).

However, two sources of uncertainty limit the precision with which temporal preparation can be deployed (temporal precision). One is the uncertainty about the passage of time. Previous work has shown that the subjective experience of time carries a degree of uncertainty that scales with the passage of time (scalar property of time; Gibbon, 1977). We thus experience a distorted

version of the veridical passage of time, and it is thought that this distortion arises from variability intrinsic to the nervous system, which furthermore scales with the duration of the stimulus to be represented (Beck, Ma, Pitkow, Latham, & Pouget, 2012). This property is also invoked to account for Weber's law in sensory systems (Barlow, 1964) and, for its temporal counterpart, the scalar property of time that links the distortion of the subjective experience of time to the duration to be estimated (Buhusi & Oprisan, 2013). Consequently, longer durations will be associated with higher internal uncertainty about how much time has actually passed. The other source of uncertainty is external and arises simply from variability in the time of occurrence of events (Beck et al., 2012).

It has long been recognized that the processing of time durations within the range of hundreds of milliseconds (interval timing) strongly depends on dopaminergic (DA) transmission (Coull, Cheng, & Meck, 2011; Matell & Meck, 2004). For example, healthy individuals show abnormal performance in timing tasks after pharmacological DA blockade (Lustig & Meck, 2005; Rammsayer, 1989). Moreover, interval timing is impaired in Parkinson disease patients who are off medication, but this impairment normalizes after levodopa administration (Praagstra & Pope, 2007; Artieda, Pastor, Lacruz, & Obeso, 1992). Indirect

¹University College London, ²University of Birmingham

evidence from healthy human participants (Tomasi, Wang, Studentsova, & Volkow, 2014; Rammsayer, 1997) and Parkinson disease patients (Smith, Harper, Gittings, & Abernethy, 2007) suggests that a specific role for DA might be in controlling levels of temporal precision (and thus its inverse, temporal uncertainty). These findings side with theoretical (Frank, 2005) and physiological (Rolls, Thorpe, Boytim, Szabo, & Perrett, 1984) observations of an increased level of neural variability after DA depletion. This line of thought has been applied to investigate the impact of DA imbalance on action reprogramming (Bestmann, Ruge, Rothwell, & Galea, 2015; Friston et al., 2012; Galea, Bestmann, Beigi, Jahanshahi, & Rothwell, 2012) and to account for Parkinsonian symptoms (Frank, 2005). However, with regard to the precision of temporal representations and temporal expectations, and how they influence our ability to prepare actions, the role of DA has never been assessed.

The present work is the first to directly address this question by comparing the impact of systemic DA blockade (haloperidol and sulpiride) on temporal preparation in healthy humans. Both DA antagonists were chosen because of their different pharmacological properties (Galea et al., 2012). Whereas sulpiride selectively blocks DA receptors of the D2 receptor family (O'Connor & Brown, 1982), haloperidol blocks both D1 and D2 receptor families (Zhang & Bymaster, 1999). Pharmacological studies on rats suggest that different DA receptor families might mediate distinct aspects of temporal preparation. D2 signaling, particularly in the striatum, is implicated in forming temporal expectations about stimulus occurrence across trials (Meck, 2006). Mesocortical D1 signaling, instead, is required to continually update the temporal representations of time accumulating within a trial (Parker, Alberico, Miller, & Narayanan, 2013).

Thus, possible differential effects of haloperidol and sulpiride on temporal preparation could pinpoint the role of D1 and D2 signaling in the formation of temporal representations and temporal expectations in humans. Specifically, a selective impact of haloperidol would provide indication for the additional relevance of D1 signaling, whereas a comparable effect of both drugs on the formation of temporal expectations would point toward the importance of D2 signaling. Moreover, in the latter case, a stronger impact of haloperidol would speak to a crucial role of nigrostriatal D2 receptors, given the specific receptor affinity of haloperidol (Coull et al., 2011).

To this end, we assessed temporal preparation using a simple variable foreperiod (FP) task. Here, the response speed ($RS = RTs^{-1}$) provides an index for the ability to deploy temporal preparation, such that more precise temporal preparation generates faster RS (Niemi & Näätänen, 1981). Specifically, two robust phenomena have been reported in variable FP experiments. First, temporal preparation is best when FP duration can be anticipated (Coull & Nobre, 1998; Karlin, 1959), whereas high FP variability renders it more difficult to prepare in

anticipation of the forthcoming event (Drazen, 1961; Klemmer, 1956). Second, within a block of trials, RSs are slowest for the shortest FPs and decrease proportionally to FP duration, a feature known as the “FP effect” (Niemi & Näätänen, 1981; Bertelson & Tisseyre, 1969; Klemmer, 1956). Importantly, these two effects can be linked to the formation of temporal expectations about stimulus occurrence across trials and to the updating of such expectations within a trial through temporal representations of the accumulating time. We adopted two model-free metrics to dissect how DA might affect the precision of temporal expectations and representations, respectively: temporal bias and temporal sensitivity.

First, the discrepancy (temporal bias) between the point in time when participants expect the appearance of the stimulus (as revealed by fastest RS) and the actually observed most likely time of appearance (i.e., the mean of the FP distribution) indexes the precision of temporal expectations across trials. By changing between-trial FP variability across blocks, we manipulated external temporal uncertainty and, thus, the degree with which participants should be able to form precise temporal expectations. The precision of temporal expectations should thus be inversely related to the degree of external temporal uncertainty (i.e., large biases for high external temporal uncertainty).

Second, the steepness of the FP effect quantifies the change in temporal preparation per unit change in FP duration, which can be conceptualized as the precision of temporal representations (temporal sensitivity). By varying the blockwise mean FP duration, we manipulated internal temporal uncertainty levels and thus the sensitivity with which participants should be able to track the passage of time. The precision of temporal representations should thus have a negative relationship with the degree of internal temporal uncertainty (i.e., less temporal sensitivity for high internal temporal uncertainty).

Previous behavioral work has investigated both internal and external uncertainties separately (e.g., Piras & Coull, 2011; Tsunoda & Kakei, 2011). However, in many situations in daily life, both forms of uncertainty occur. Our task allows for investigating how both internal and external temporal uncertainties affect temporal preparation and how this influence in turn is controlled by DA. In addition, we employed a model-based analysis to estimate the contribution of DA on subjective temporal uncertainty. The subjective hazard function incorporates the scalar property of time and has been successfully employed to model temporal preparation in monkeys (Janssen & Shadlen, 2005) and humans (Tsunoda & Kakei, 2011). Specifically, it describes the time profile for the probability of occurrence of an imperative event (see Methods for details). The marginal and conditional probability terms of this function capture temporal expectations across trials and temporal representations within trial, respectively. Subjective uncertainty is captured formally by the Weber fraction of the subjective hazard function

(e.g., a small Weber fraction indicates low subjective uncertainty; Janssen & Shadlen, 2005). By estimating the Weber fraction separately for the marginal and conditional probability, we were able to measure the subjective uncertainty introduced by our DA manipulation with a specific focus on D1/D2 differential effects for temporal expectations and temporal representations.

This study thus provides novel evidence for the role of DA in controlling the precision of temporal preparation for motor responses in healthy humans. Our results show that the precision of temporal preparation reduces with increasing temporal uncertainty and that DA blockade produces an overall slowing of RS. However, haloperidol affected both the formation of temporal expectations (i.e., extraction of the mean FP) across trials and the precision of the temporal representations encoding the elapsed time within a trial. Specifically, these impairments appeared under conditions of high levels of external and internal temporal uncertainties. A fitting of the subjective hazard function (Janssen & Shadlen, 2005) to the empirical RS data confirmed that these effects were caused by an overall increase in subjective temporal uncertainty as indicated by large estimated Weber fractions. Moreover, such increase in subjective temporal uncertainty was maximal under haloperidol. Conversely, neither the precision nor accuracy of movements was affected by DA depletion, indicating a dissociable influence of DA on temporal and motor functions.

METHODS

Participants

Seventeen healthy human volunteers (eight men, nine women) aged between 23 and 37 years (mean age = 27.5 ± 3.9 years) participated in this study. They had normal or corrected-to-normal vision, and none of them had a history of neurological disorder or drug abuse. The suitability of the participants for the pharmacological protocol was evaluated based on review of their clinical history by a neurologist (D. R.). All volunteers were naive to the experimental aims, provided written informed consent, and received monetary compensation for their time and travel (£15 per session). Experimental protocols conformed to the guidelines of the Declaration of Helsinki and were approved by the research ethics committee of University College London.

Pharmacological Protocol

The experiment was conducted in a double-blind, placebo-controlled, crossover design. Drug administration was randomized and counterbalanced across participants. In every experimental session, participants were administered by a medically trained individual (D. R.) a single oral dose of either 2.5 mg of haloperidol, 400 mg of sulpiride, or

placebo (Bestmann et al., 2015; Lake & Meck, 2013; Frank & O'Reilly, 2006; Rammsayer, 1997). The behavioral task was performed 2 hr after drug ingestion to coincide with the peak plasma concentration of the drugs (Korchounov & Ziemann, 2011; Deleu, Northway, & Hanssens, 2002). Experimental sessions were separated by at least 1 week to allow systemic drug clearance before the next drug intake. After completion of every session, participants reported whether they thought they received an active drug or a placebo as well as their overall levels of attention and fatigue experienced during the experiment.

Apparatus and Stimuli

Participants made planar reaching movements with their dominant arm while holding the handle of a robotic manipulandum (Figure 1A). They were seated leaning slightly forward, with their forehead supported by a gel cushion. Movements were constrained in the horizontal plane and performed at chest height. An arm brace was used to reduce unwanted wrist movement, whereas movements of the trunk, shoulder, and elbow were not constrained. An LCD monitor (refresh rate = 60 Hz) was mounted horizontally above the experimental setup. Participants viewed the reflection of the monitor in a mirror suspended above the manipulandum. In this way, visual feedback was projected into the plane of movement, and direct vision of the arm was prevented. The position of the arm was measured by sensors placed on the handle of the robotic manipulandum at a sampling rate of 200 Hz and indicated in real time by an unfilled cursor (0.3 cm in diameter) on the display. The experimental computer (Precision T3500, quad-core 2.8 GHz, 100-GB RAM; Dell Computer Corp., Austin, TX) processed this information online using C++ custom-written routines. The starting point and the target of the movement were represented by two equally sized squares (1 cm) shown on a black background, positioned along participants' medial line (between squares, distance = 6 cm).

Behavioral Task

Before each trial, participants placed the white cursor into the center of the starting square by moving the robotic manipulandum (see Figure 1A and B). The trial started once the participant had maintained the cursor within a radius of 0.3 cm from the center of the starting square for 300 msec. After this, the target square turned blue (warning stimulus, WS) and indicated the impending appearance of the imperative stimulus (IS; green target square). The onset of the IS prompted participants to respond as quickly as possible, but not at the expense of accuracy, by moving their arm in a "shooting" fast movement aiming at the center of the target cursor. The arm cursor disappeared at the onset of the WS so that the movement was performed without visual guidance to discourage online movement corrections. At

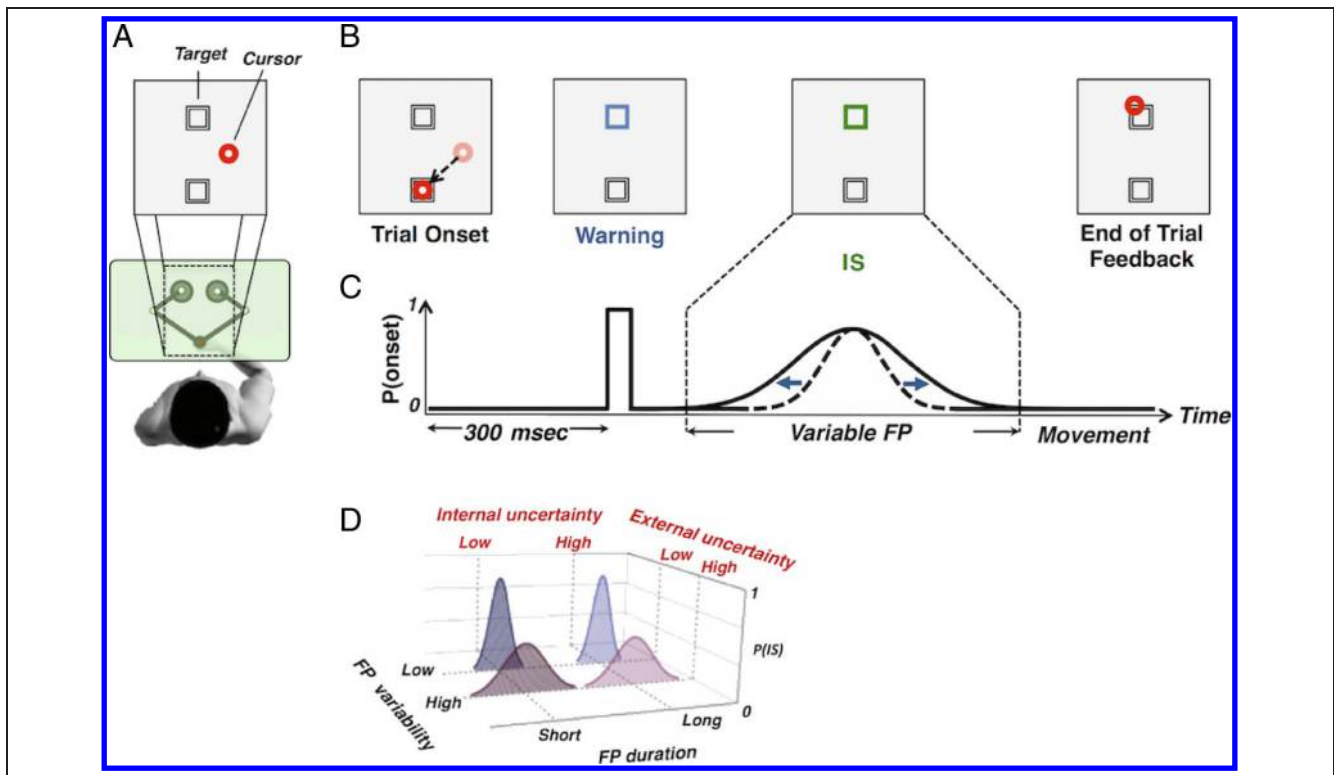


Figure 1. Variable FP task and manipulation of temporal uncertainty. (A) Participants made planar reaching movements to a target square while holding a robotic manipulandum. They viewed the reflection of the monitor in a mirror suspended above the manipulandum. In this way, visual feedback was projected into the plane of movement, and direct vision of the arm was prevented. (B) Movement was instructed by the color of the target square. After a WS (blue target square), the onset of the IS (green target square) after a variable FP required a fast movement to the target square. (C) Internal and external temporal uncertainties were manipulated by changing the mean and variance of the time between the WS and IS (FP) across blocks. In each block, FPs were drawn from a truncated Gaussian distribution, with mean μ and standard deviation σ . (D) Four different distributions were used in a blocked factorial design: μ (short, long) \times σ (low, high) corresponding to Internal temporal uncertainty (low, high) \times External temporal uncertainty (low, high).

the end of the movement (defined by the distance from the starting square larger than 3 cm and speed lower than 3.5 cm/sec), visual feedback was given in the form of a stationary red cursor, which appeared at the location of the movement end point and lasted for 1 sec.

Experimental Design and General Procedure

On each trial, the FP duration was randomly sampled from a truncated Gaussian distribution (see Figure 1C and D). In a blocked 2×2 factorial design, we manipulated mean FP duration (short: 1500 msec, long: 3000 msec) and FP variability (i.e., standard deviation; low: 100 msec, high: 600 msec). The two distributions for short FPs were truncated at 500 msec, here considered as the minimum time required for preparation (Hackley et al., 2009), and at 2500 msec (longest FP) to preserve the distribution's symmetry. To ensure comparable standard deviations between short and long distributions, both tails were also truncated to the long distribution at 2000 and 4000 msec. The variable FP duration required participants to form an estimate of the most likely FP (the mean of the adopted FP distribution) for a given block. Hence, such an estimate would suffer from the uncertainty introduced by

increasing FP variability. In addition, longer mean FP duration increases temporal uncertainty because timing accuracy deteriorates proportionally to the duration of the time interval (Gibbon, 1977). Consequently, participants should respond faster for FP durations closer to the mean FP, whereas increasing FP variability and mean FP duration should diminish this gain in RS.

The experiment was composed of one training session and three experimental sessions. Each experimental session consisted of four blocks of 110 trials each, separated by a short rest. A training block of 60 trials was conducted before the main experiment, and each block started with 20 warm-up trials. Both the training block and the warm-up trials were identical to the experimental counterparts, but with the FP sampled from an exponential (non-aging) distribution with a mean of 1000 msec. Participants could therefore practice the task without being exposed to the changes in conditional probability over the course of the trial (i.e., the hazard rate) in the main experiment. The order of conditions (blocks) was balanced across sessions and participants following a Latin square design. Excluding training and warm-up trials, 1320 experimental trials (3 sessions \times 4 blocks \times 110 experimental trials) were collected for each participant.

At completion of each session, participants assessed their attention level, fatigue, and quality and amount of sleep for the previous night using a 7-point Likert scale where 1 and 7 represented the minimum and maximum ratings, respectively (e.g., 1 = *poorest quality of sleep* and 7 = *highest quality of sleep*).

Data Preprocessing

Movement start and end were defined as the time points when velocity exceeded and fell below 3.5 cm/sec. RTs were calculated as the delay between the onset of the IS and movement onset. Trials outside the minimum–maximum RT (100 msec < RT < 2000 msec), maximal end-point distance (>6 cm from the distal square), or outlier (msec, mean \pm 3 SDs; Ratcliff, 1993) criteria (4.4% total) were excluded from further analysis.

Temporal Preparation: Model-free Analyses

RS

We analyzed mean RS (1/RT; Ratcliff, 1993) as a measure of temporal preparation. Previous work has reported increased intraindividual variability in response latencies associated with DA depletion (Burton, Strauss, Hultsch, Moll, & Hunter, 2006; Reed & Franks, 1998). A general increase in response variability should reduce RS regardless of the levels of temporal uncertainty introduced by the experiment. To control for this possibility, we analyzed within-participant RS variability by calculating the coefficient of variation (CV, ratio between the standard deviation and the mean RS of the sample; Goldstone, 1968).

Temporal Bias and Sensitivity

Because preparation (and thus RS) increases with time (Niemi & Näätänen, 1981), the fastest responses are likely to occur for FPs at the end of the distribution. A detrending procedure subtracted the best-fit linear trend as a function of FP (see Figure 2C, left). In this way, residual values allow for calculating the FP corresponding to the maximum RS independently from slow changes in temporal preparation with the passage of time (Figure 2C, right). Specifically, the bias in temporal expectation was quantified for each block as the difference between the FP at which the maximum RS occurred on average and the mean of the actually sampled FP distribution. The smaller the bias, the better participants learned about the average FP duration. Conversely, the slope of the subtracted linear fit quantifies the change in temporal preparation per unit change in FP duration (i.e., sensitivity). A robust FP effect would correspond to large positive slopes (because $RS = RT^{-1}$) and thus would indicate faster RS for longer FP within a block.

Temporal Preparation: Model-based Analyses

Modeling Temporal Expectation: Subjective Hazard Function

The hazard function describes the time profile for the probability of occurrence of the IS and is defined as the marginal probability that an IS will appear at a given time, divided by the conditional probability that it has not yet occurred:

$$H(t) = \frac{f(t)}{1-F(t)} \quad (1)$$

where $f(t)$ is a probability density function with the same mean and standard deviation of the FP distribution for a given block and $F(t)$ is the corresponding cumulative density function,

$$F(t) = \int_0^t f(t)dt \quad (2)$$

Marginal and conditional probabilities reflect the probability of a stimulus occurrence across trials and within the current trial, respectively. Hence, they can be considered as models of temporal expectation and temporal representations. However, the formulation of the hazard function does not take into account the subjective temporal uncertainty that scales with the duration of the interval of time (Gibbon, 1977). Such uncertainty implies that participants experience a distorted version of the veridical FP distribution (Figure 3B). With this in mind, we calculated the subjective hazard function (Tsunoda & Kakei, 2011; Janssen & Shadlen, 2005) by first smoothing the probability density function $f(t)$ with a Gaussian distribution whose standard deviation scaled with the duration of the interval of time (Figure 3C and D). This is similar to convolution, but it fails shift invariance as it “blurs” the later points more than the earlier points, which reflects the increased uncertainty for longer durations. As a result, we obtained the distribution of “subjective” FPs.

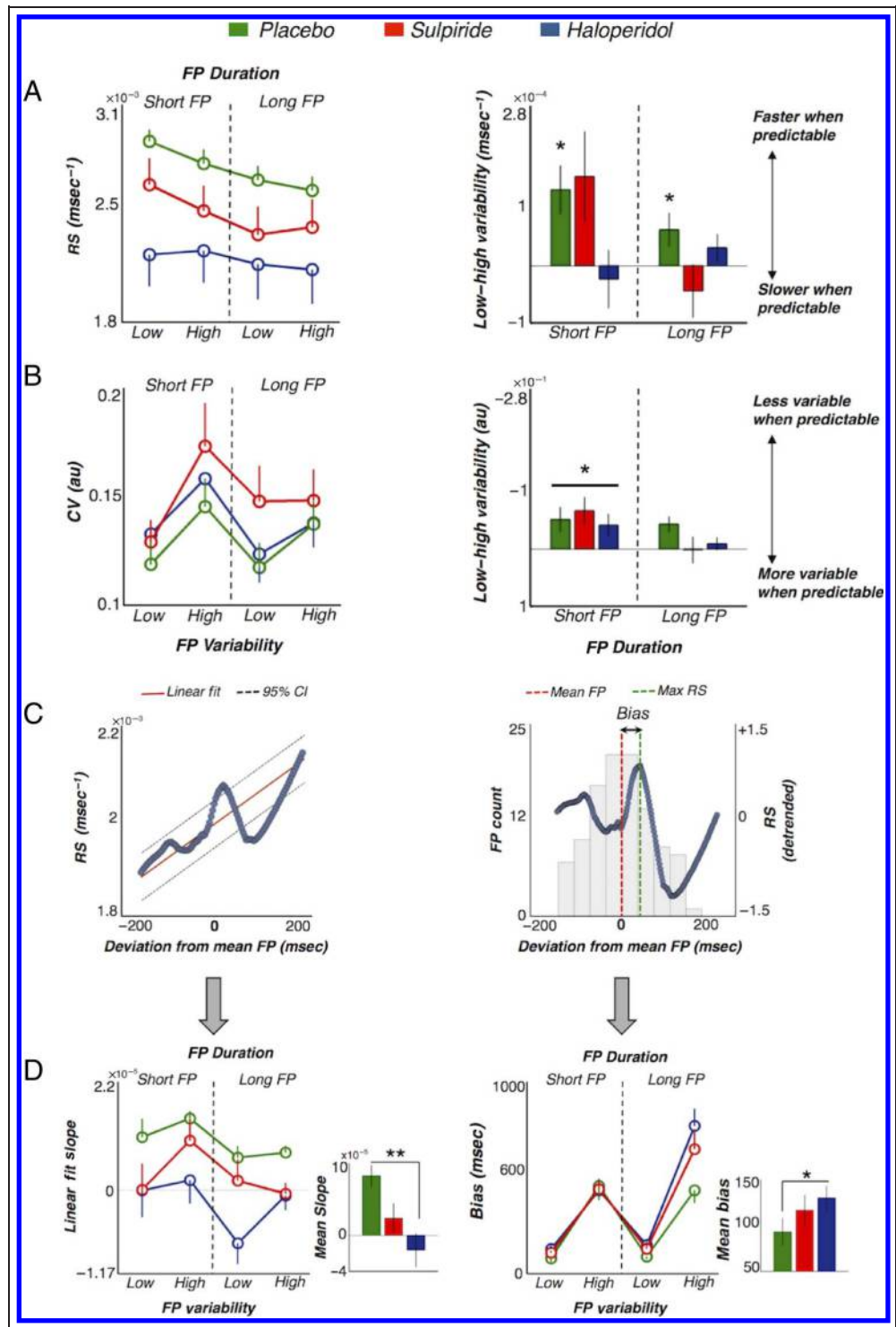
$$\tilde{f}(t) = \frac{1}{\phi t \sqrt{2\pi}} \int_{-\infty}^{+\infty} f(s) e^{\frac{(s-t)^2}{2\phi^2 t^2}} d(s) \quad (3)$$

where ϕ corresponds to the Weber fraction for time estimation. By substituting Equation 3 and its definite integral in Equation 2, we obtain the subjective hazard function

$$\tilde{H}(t) = \frac{\tilde{f}(t)}{1-\tilde{F}(t)} \quad (4)$$

The Weber fraction provides a measure for the precision of temporal preparation. For instance, small Weber fractions correspond to steep subjective hazard functions, whereas with larger Weber fractions, the increase in the subjective hazard function for longer FP is more gradual (Figure 3E). Here, we estimated two Weber fractions, one for the marginal and one for the conditional probabilities of the subjective hazard function. In previous work that has employed the subjective hazard function to study

Figure 2. Temporal preparation and dopamine: model-free analysis. (A, left) Average median RS (msec^{-1}) for each level of FP variability (bottom abscissa) and FP duration (top abscissa). Placebo: green, sulpiride: red, haloperidol: blue. (Right) Changes in RS between low and high FP variability conditions, plotted against FP duration. (B, left) CV of RS for each level of FP variability (bottom abscissa) and FP duration (top abscissa). (Right) Changes in RS variability between low and high FP variability conditions, plotted against FP duration. (C, left) Because temporal preparation increases with the passage of time, the fastest responses are likely to occur for long FP durations. A detrending procedure subtracted the best-fit linear trend as a function of FP. Because temporal preparation is also based on the updating of the conditional probability of an event over the course of time, the slope of the fitted linear trend is a measure of the temporal sensitivity of such process. (Right) The temporal distance (absolute error) from the residuals' peak time (green dashed line) and the mean FP (red dashed line) indicate how much temporal preparation was misaligned to the mean stimulus onset (i.e., the temporal bias). Gray background histogram: distribution of FPs for an illustrative session from a single participant. Plots present data from a representative participant. (D, left) Resulting positive slopes indicate a normal FP effect under placebo, with RS increasing with FP duration. (Right) Response bias and temporal uncertainty. (Inlay) Data collapsed across conditions. Error bars represent $\pm 1 \text{ SEM}$. One and two asterisks indicate significance at the $p \leq .05$ and $p \leq .01$ levels, respectively.



temporal preparation (e.g., Bueti, Bahrami, Walsh, & Rees, 2010; Janssen & Shadlen, 2005), a constant time delay, τ , was used to account for delays in the responses introduced by temporal uncertainty (Janssen & Shadlen, 2005) so that $\tilde{H}(\tau + t)$. We considered the possibility that the time delay τ changed with DA blockade. Moreover, given empirical evidence suggesting that two independent processes could operate during a variable FP task (Tsunoda & Kakei,

2011; Karlin, 1959), we also treated the $\tilde{f}(t)$ and $\tilde{F}(t)$ of the hazard function as two separate components with independent parameters ϕ_1 and ϕ_2 , respectively.

We fitted four models each with a different set of free parameters (M1: τ , ϕ_1 , and ϕ_2 ; M2: ϕ_1 and ϕ_2 ; M3: τ and ϕ ; M4: ϕ ; see also Figure 4A), and then, for the model comparison, we used random effects Bayesian model selection (Stephan, Penny, Daunizeau, Moran, & Friston, 2009) to

choose the most likely model given the observed RS data. The resulting exceedance probability indicated the likelihood of each model to be the most frequently occurring model in the comparison set, and the mean of the posterior distribution provides an estimate of the frequency with which any model occurs in the population. Model comparison showed that a model including two Weber fractions ϕ_1 and ϕ_2 as free parameters (M2) had the highest exceedance probability (M2 exceedance probability: placebo, 0.99; sulpiride, 1; haloperidol, 0.98) and largest mean posterior (M2 mean posterior probability: placebo, 0.66; sulpiride, 0.72; haloperidol, 0.6) to generate the data of any randomly selected participant (Figure 4A). A between-comparison (Rigoux, Stephan, Friston, & Daunizeau, 2014) confirmed that the same model best explained our data for all treatment conditions (probability that model frequencies differ between drugs, $p < .001$). Hence, from here onward, we will only refer to this model.

Subjective Hazard Model Fitting and Model Comparison

RSs were smoothed to assist the model fitting. A robust lowess filter (span = 0.3) was used for reducing uncer-

tainty while preserving the overall shape of RS over time. We fitted Equation 4 to the smoothed RS of our participants and estimated the Weber fractions ϕ_1 and ϕ_2 of the model $\tilde{f}(t)$ and $\tilde{F}(t)$, respectively. We used a least squares regression to fit the model to the RS data. A multistart optimization algorithm was adopted to search efficiently for the global minimum of the regression hypersurface (MATLAB multistart function). Start points were chosen randomly, with a lower bound of zero to avoid negative values. For the model comparison, sum of squared errors was converted into log-likelihood and then used to calculate Akaike information criterion scores. Such scores were then submitted to random effects Bayesian model selection (Stephan et al., 2009).

Reaching Movements

Kinematics

Kinematic data were analyzed off-line with custom written MATLAB (The MathWorks, Natick, MA) routines. For each trial, arm trajectories were computed and filtered with a fourth-order two-way 20-Hz low-pass Butterworth filter. All trajectories were further inspected manually.

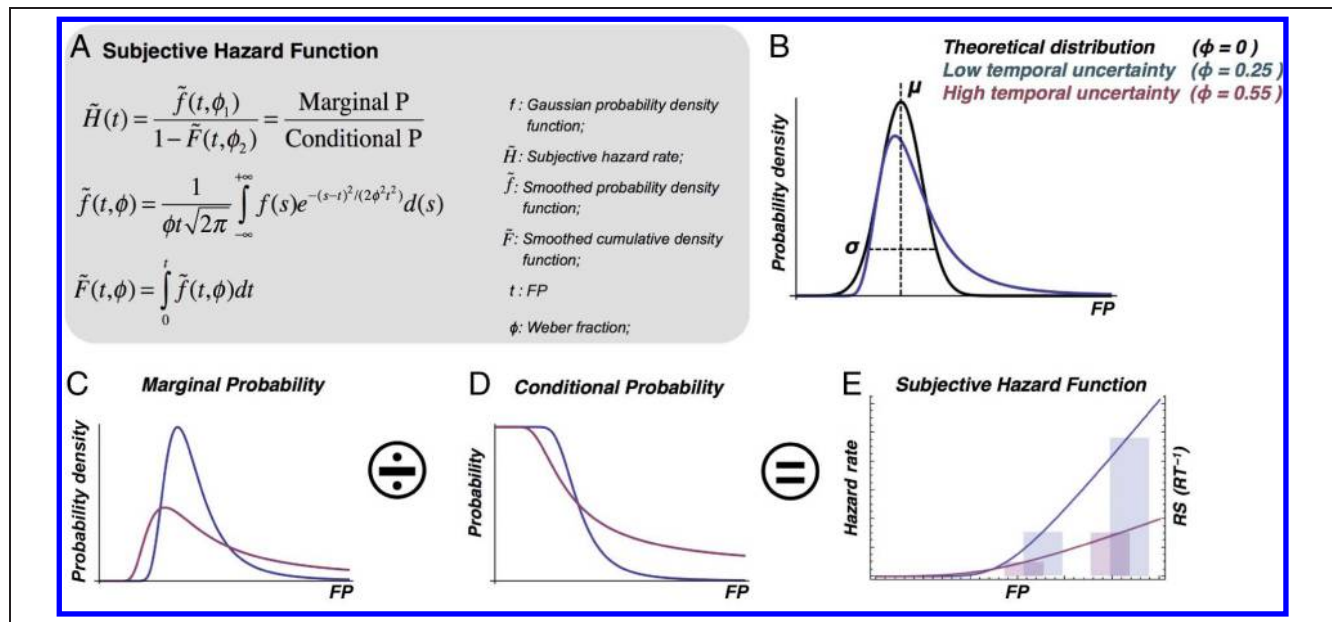


Figure 3. Temporal preparation and subjective temporal uncertainty: the subjective hazard function. (A) The subjective hazard function formalizes the overall probability of the appearance of a stimulus at a given time by taking into account both the marginal probability of the stimulus and its increase in conditional probability with the passage of time. The smoothing parameter ϕ corresponds to the Weber fraction for time estimation and provides a measure for the subjective uncertainty in experiencing time (Janssen & Shadlen, 2005). (B) Subjective temporal uncertainty implies that participants experience a distorted version (blue) of the actual FP distribution (black) with mean μ and standard deviation σ . Subjective temporal uncertainty scales with the elapsed interval of time (scalar property of time) as shown by the right heavy tail of the experienced distribution. ϕ values arbitrarily chosen for illustration purposes. (C) Subjective marginal probability that a stimulus will appear at time t . In this example, the distributions have same μ and σ but different smoothing parameters ϕ , with the magenta indicating larger ϕ values (i.e., larger Weber fractions) and thus higher subjective temporal uncertainty. High subjective temporal uncertainty produces a shift (i.e., a bias) in the expectation about the most likely time of stimulus occurrence (i.e., the curve peak). (D) Subjective conditional probability that a stimulus will occur given that it has not occurred already. High subjective temporal uncertainty reduces the slope of the conditional probability function reflecting a diminished impact of the passage of time on forming expectations about the time of stimulus occurrence. (E) Hypothesized relationship between subjective hazard function and RS for different levels of subjective temporal uncertainty. Higher levels of subjective temporal uncertainty reduce temporal preparation, resulting in a shallower hazard function and slower responses (magenta).

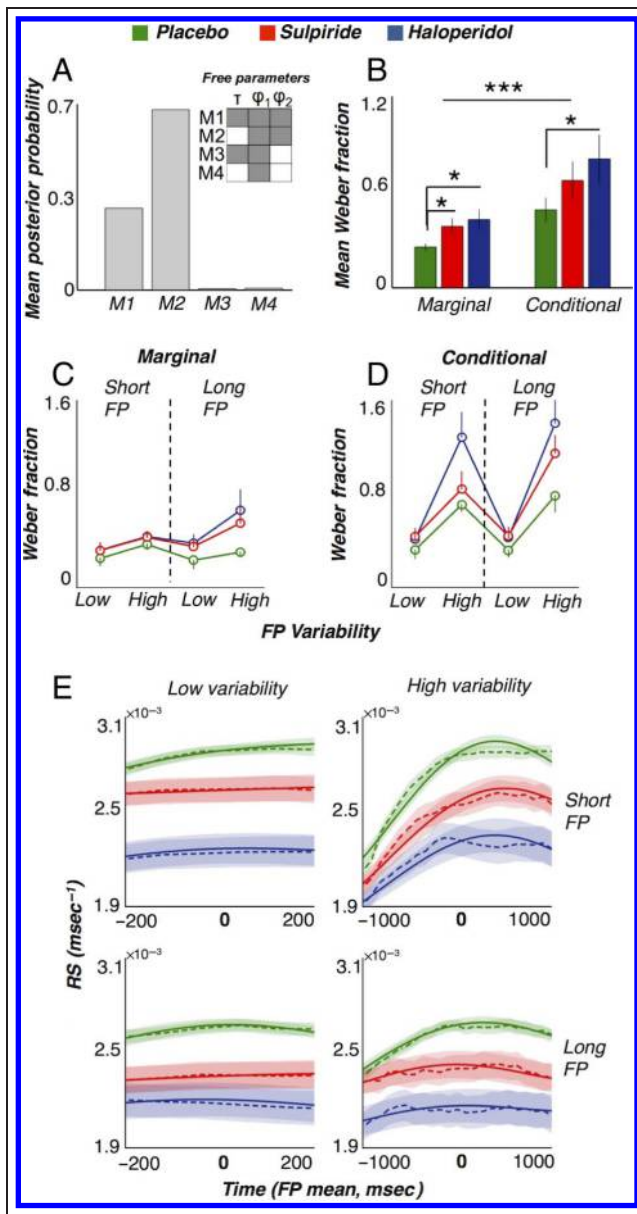


Figure 4. Model comparison, estimated Weber fractions, and model fits. (A) Random effects Bayesian model selection of subjective hazard models with different free parameters. M1: variable time delay and independent Weber fractions for the marginal and conditional components. M2: independent Weber fractions for the marginal and conditional components. M3: variable time delay and one shared Weber fraction. M4: one shared Weber fraction. The bars show that the mean posterior probability that M2 generated the data of any randomly selected participant was the highest. (B) Weber fractions estimated from the winning model (M2) and collapsed across external and internal temporal uncertainties quantify the degree of subjective temporal uncertainty. (C and D) Weber fractions separated by external and internal temporal uncertainties. (E) Averaged RS profiles (dashed lines) and model fits (solid lines) from the model are superimposed for comparison. Lines are aligned with respect to the mean of the FP distribution (i.e., Time 0 on the abscissa; placebo: green, haloperidol: blue, sulpiride: red). Error bars and shaded areas represent ± 1 SEM. One and three asterisks indicate significance at the $p \leq .05$ and $p \leq .001$ levels, respectively.

Trajectories and velocity profiles were aligned on their starting points before averaging. Reaching accuracy and precision were assessed by fitting 95% confidence ellipses to movement end points. The semimajor and semiminor axes and the orientation of the ellipses were computed from the first and second principal component analyses of the end-point scatter. From these axes, confidence ellipses encompassing 95% of end-point population were constructed. The position of the ellipses' centroid with respect to target position gives a measure of reaching accuracy, whereas its area (more precisely, its reciprocal) provides an overall measure of precision (Revol et al., 2003).

Statistical Analysis

Repeated-measures ANOVA (rm-ANOVA) was adopted to assess statistical significance of our results across Medication (placebo, haloperidol, sulpiride), FP duration (short, long), and FP variability (low, high) in a full factorial within-participant design. Specifically, the same statistical analysis was conducted separately for mean RS, RS variability (CV), temporal bias, and temporal sensitivity and on kinematic parameters (peak velocities of reaching movements, movement times, end-point accuracy and precision).

The same approach was used to analyze Weber fractions estimated from the model fitting by analyzing the estimates for the marginal and conditional components separately. Because we found no significant interactions between drugs, we collapsed the FP duration and variability to assess the effects of drugs on the two components. Hence, in this case, the rm-ANOVA had Drugs (placebo, haloperidol, sulpiride) \times Components (marginal, conditional) as factors.

We report partial η^2 (η_p^2) as a measure of main effect size and Cohen's d_z (Cohen, 1988) for the effect size of post hoc t test comparisons. Corrections for multiple comparisons were performed using Bonferroni correction. The effectiveness of the blinding protocol was assessed with the Friedman's test on postsession questionnaire scores. For all analyses, the level of statistical significance was fixed at .05. Unless stated otherwise, all data shown represent mean \pm SEM.

RESULTS

Blinding

No side effects associated with the drug administration were reported. Questionnaire scores did not differ between sessions for the participants' rating of attention (1 = *poor*, 7 = *excellent*; placebo: 4.82 ± 0.38 , sulpiride: 4.94 ± 0.36 , haloperidol: 4.71 ± 0.21 ; $\chi^2 = 1.39$, $df = 2$, $p = .49$) or fatigue (1 = *low*, 7 = *high*; placebo: 3.12 ± 0.38 , sulpiride: 2.88 ± 0.32 , haloperidol: 3.47 ± 0.42 ; $\chi^2 = 1.12$, $df = 2$, $p = .57$) as revealed by Friedman's test.

Furthermore, only 4 of 17 (23%) participants correctly identified the placebo session, confirming the effectiveness of the blinding protocol.

Temporal Preparation: Model-free Analyses

Mean RS

Participants were able to perform the task without difficulty as revealed by the low error rates observed for the entire experiment (4% of total responses). We assessed possible effects of DA on responses by splitting the error trials into premature and late responses. Across all conditions, neither the percentage of premature or late responses differed significantly between drug conditions (Friedman's test, premature: $\chi^2 = 16.09$, $df = 11$, $p = .14$; late: $\chi^2 = 17.19$, $df = 11$, $p = .1$).

We then explored the effect of uncertainty on RS under the influence of DA blockade. Figure 2 (A and B) shows the averaged RS and variability for each drug condition and uncertainty level. Under placebo, RSs were faster for FP distributions with a short mean ($F(1, 16) = 22.179$, $p < .001$, $\eta_p^2 = 0.581$) and low variability ($F(1, 16) = 5.781$, $p = .029$, $\eta_p^2 = 0.265$), indicating increased temporal preparation for low internal and external uncertainty conditions.

DA blockade resulted in a general slowing of RS ($F(2, 32) = 7.046$, $p = .003$, $\eta_p^2 = 0.306$), relative to placebo. However, this slowing was statistically significant only for haloperidol ($t(32) = 2.449$, $p = .02$, $d_z = 0.59$). A significant three-way interaction revealed that the beneficial effect of low FP variability and short FP duration on temporal preparation was influenced by the DA treatment ($F(2, 32) = 3.308$, $p = .049$, $\eta_p^2 = 0.171$). Under placebo, uncertainty significantly modulated RS (short FP: $t(32) = 3.17$, $p = .006$, $d_z = 0.77$; long FP: $t(32) = 2.1$, $p = .05$, $d_z = 0.51$). By contrast, under the effect of medication, the effect of FP variability was no longer significant (sulpiride: short FP, $t(32) = 1.97$, $p = .066$, $d_z = 0.48$; long FP, $t(32) = 0.95$, $p = .352$, $d_z = 0.23$; haloperidol: short FP, $t(32) = 0.45$, $p = .652$, $d_z = 0.11$; long FP, $t(32) = 1.24$, $p = .223$, $d_z = 0.3$).

We also tested whether RS variability, measured as CV (RS standard deviation/RS mean), was affected by our drug manipulations. If the capacity to anticipate events was altered because of an overall increase in behavioral variability, one would expect generally more variable responses under DA blockade, regardless of FP variability. Under placebo, RS variability increased with FP variability ($F(1, 16) = 11.312$, $p = .004$, $\eta_p^2 = 0.414$) in that responses were more variable when FP variability was high (Figure 2B). This effect was reduced to nonsignificant levels for long FPs (FP duration \times FP variability: $F(1, 16) = 5.455$, $p = .033$, $\eta_p^2 = 0.254$; post hoc: short FP, $t(16) = 4$, $p = .002$, $d_z = 0.97$; long FP, $t(16) = 1.71$, $p = .12$, $d_z = 0.41$). Importantly, RS variability was not affected by DA intervention ($F(2, 32) = 2.281$, $p = .119$, $\eta_p^2 = 0.125$).

Although participants showed slower RS under DA blockade, their variability was not significantly different from placebo (Figure 2B, right). Impaired temporal preparation therefore cannot be accounted for by a general, unspecific increase in behavioral variability.

Temporal Bias and Temporal Sensitivity

To better characterize the impact of our manipulations on temporal preparation, we adopted two distinct model-free metrics: bias in temporal expectation and the sensitivity of temporal representations. The independence of such measures was assessed by a correlation analysis between the size of temporal biases and temporal sensitivity (placebo: $r = .21$, $p = .08$; sulpiride: $r = .002$, $p = .98$; haloperidol: $r = .16$, $p = .18$).

Temporal Bias

To assess whether the altered temporal preparation under DA blockade was caused by an impaired ability to form temporal expectations, we measured individual temporal bias, here defined as the (absolute) temporal difference between the peak of the RS curve and the mean of the FP distribution (Figure 2C, right). In this metric, temporal preparation is optimal when one's temporal expectation is aligned to the actual onset of the stimulus or, in other words, when temporal biases are minimal.

Similar to mean RS, temporal bias (Figure 2D, right) was smaller for FP distributions characterized by short mean ($F(1, 16) = 9.531$, $p = .007$, $\eta_p^2 = 0.373$) and low variability ($F(1, 16) = 217.468$, $p < .001$, $\eta_p^2 = 0.931$). DA blockade resulted in significantly larger temporal biases ($F(2, 32) = 4.188$, $p = .024$, $\eta_p^2 = 0.207$; errors [mean \pm SEM]: placebo, 92.9 ± 7.5 msec; sulpiride, 116.5 ± 10.8 msec; haloperidol, 129.88 ± 7.9 msec) relative to placebo, although only haloperidol proved statistically significant as revealed by follow-up analysis ($t(32) = 3.78$, $p = .008$, $d_z = 0.92$). This pattern of results points toward an impaired ability to correctly anticipate the IS onset when under the influence of haloperidol.

Temporal Sensitivity

Temporal preparation also changes with the changes in conditional probability of an event over the course of time. The slopes of the RS profiles against FP durations (Figure 2C, left) capture the sign and the temporal sensitivity of these changes. This provides a measure for the precision of temporal representations. In this metric, optimal temporal preparation implies a precise representation of the passage of time and thus large positive slopes of the RS profiles.

Our analysis revealed that the temporal sensitivity of the FP effect was indeed influenced by FP duration

(Figure 2D, left), with significantly smaller slopes associated to blocks with long mean FPs ($F(1, 16) = 12.191, p = .003, \eta_p^2 = 0.432$). This pattern was inverted for FP variability, where more variable FP blocks yielded significantly larger slopes ($F(1, 16) = 4.188, p = .021, \eta_p^2 = 0.289$). Higher FP variability implies that more FPs are drawn from the end of the distribution yielding faster responses (i.e., the FP effect). At the same time, it also indicates that the precision of temporal representations is affected by internal uncertainty, which increases with the duration of the FP. The slopes of the RS profiles differed significantly across drug conditions ($F(2, 32) = 6.149, p = .005, \eta_p^2 = 0.278$). Under placebo, participants showed the expected FP effect as indicated by a positive slope for all conditions (note that slope is positive because we used RS, which is the inverse of RTs; mean \pm SEM = 0.099 ± 0.011). Slopes were, on average, smaller under sulpiride (mean \pm SEM = 0.028 ± 0.035) and negative for haloperidol (mean \pm SEM = -0.025 ± 0.035), but this effect was significant only for haloperidol, when compared with placebo ($t(32) = 3.26, p = .014, d_z = 0.79$).

From a behavioral viewpoint, this effect of haloperidol corresponded to a reversed FP effect, whereby longer FP durations yield slower RSs. A significant three-way interaction indicated that the effect of DA blockade with respect to placebo was circumscribed to long FP durations, regardless of FP variability for haloperidol (low variability: $t(32) = 3.954, p = .003, d_z = 0.96$; high variability: $t(32) = 2.718, p = .047, d_z = 0.66$), but only for high variability for sulpiride ($t(32) = 4.66, p = .001, d_z = 1.13$).

Hence, these results suggest that DA blockade reduces temporal preparation by both reducing the precision of temporal representations and temporal expectations. In particular, under sulpiride, temporal sensitivity was reduced compared with placebo only for the highest levels of internal and external uncertainties. For haloperidol, however, the effect was maximal for high levels of internal temporal uncertainty, but there was no interaction with external temporal uncertainty. The latter finding may point to saturation of the detrimental effect of DA blockade with haloperidol, such that temporal sensitivity cannot be further affected by manipulations of external temporal uncertainty. This interpretation is corroborated by the subsequent model-based analyses.

Subjective Temporal Uncertainty: Model-based Analyses

Hazard Model Fits

Precise temporal preparation is likely underpinned by two distinct mechanisms. In a variable FP task, their separate contributions integrate to form RS profiles that resemble the actual hazard function of the IS. Hence, to characterize the impact of DA blockade on these mechanisms, we fitted a subjective hazard function to individual RS data. We estimated the Weber fractions (representing

the degree of subjective temporal uncertainty) for both the marginal and conditional components of the model. This approach allows for separately estimating changes induced by DA depletion on the formation of temporal expectation across trials and the formation of temporal representations within trial. Our model accurately captured the features of the RS profiles (Pearson's $r^2 \pm$ SEM: placebo, $.73 \pm 0.029$; sulpiride, $.70 \pm 0.049$; haloperidol, $.74 \pm 0.049$; Figure 4E).

Estimated Weber Fractions

In general, under placebo, the estimated mean Weber fractions (ϕ_1 : marginal, ϕ_2 : conditional) were smaller than those under DA treatment (ϕ_1 : placebo, 0.29; sulpiride, 0.41; haloperidol, 0.45; ϕ_2 : placebo, 0.53; sulpiride, 0.71; haloperidol, 0.88), indicating higher subjective temporal uncertainty after DA blockade (Figure 4C and D). More specifically, DA depletion significantly increased the Weber fractions of both the marginal (ϕ_1 : $F(2, 32) = 5.02, p = .013, \eta_p^2 = 0.239$) and conditional (ϕ_2 : $F(2, 32) = 4.99, p = .013, \eta_p^2 = 0.238$) components of the subjective hazard function. However, post hoc analysis showed that only the marginal component was significantly altered by both drugs (ϕ_1 : sulpiride, $t(2) = 2.76, p = .021$; haloperidol, $t(2) = 2.44, p = .039$; one tailed), whereas only haloperidol impacted on the conditional component (ϕ_2 : sulpiride, $t(2) = 2.31, p = .052$; haloperidol, $t(2) = 2.73, p = .022$; one tailed) when compared with placebo.

Although the rm-ANOVA pointed to a lack of significant influence of sulpiride on the conditional component, the effect was quantitatively similar for both drug conditions. We thus maintained a cautious position toward such result, and because the rm-ANOVA did not reveal any interaction, we collapsed the estimated values across levels of external and internal temporal uncertainties to search for possible selective effect of DA blockade on the two model components.

We performed a two-way rm-ANOVA on the collapsed values with drugs (placebo, sulpiride, haloperidol) and Weber fractions (ϕ_1 and ϕ_2) as factors. The results (Figure 4B) confirmed that, under DA blockade, Weber fractions were significantly larger than those in the placebo condition ($F(1, 16) = 11.05, p < .001, \eta_p^2 = 0.408$), with the conditional component characterized by significantly larger mean Weber fractions when compared with the marginal component ($F(1, 16) = 21.28, p < .001, \eta_p^2 = 0.571$). However, the rm-ANOVA failed to identify any specific effect of DA on the two components as evidenced by the absence of interactions. Hence, the impaired temporal preparation observed in the model-free analysis can be explained by increased subjective temporal uncertainty caused by DA blockade. The pharmacological challenge appears to impact on the subjective temporal uncertainty levels of both the putative mechanisms recruited by the variable FP task, here modeled as

the marginal and conditional components of the subjective hazard function.

Reaching Movement Analysis

Given the importance of nigrostriatal regions for both movement and interval timing (Coull et al., 2011), we investigated whether DA-antagonist administration affected the precision and accuracy of reaching movement end points, under different conditions of temporal uncertainty.

End-point Accuracy and Kinematics

Participants reached for the target accurately and precisely as shown by the average distance of movement end points to the target (Figure 5C; mean \pm SEM: placebo, 0.329 ± 0.05 cm; sulpiride, 0.340 ± 0.06 cm; haloperidol, 0.329 ± 0.05 cm) and by the area of the fitted 95% confidence interval ellipses (Figure 5D; mean \pm SEM: placebo, 3.2 ± 0.75 cm; sulpiride, 3.75 ± 0.83 cm; haloperidol, 3.38 ± 0.75 cm), respectively. Neither temporal uncertainty nor DA blockade had significant effects on reaching accuracy

(DA manipulation: $p = .206$, FP duration: $p = .952$, FP variability: $p = .611$) or precision (DA manipulation: $p = .079$, FP duration: $p = .393$, FP variability: $p = .338$).

Peak velocities (Figure 5E) were not significantly affected by any of our manipulations (mean \pm SEM: placebo, 47.8 ± 3.76 cm/sec; sulpiride, 48.4 ± 4.06 cm/sec; haloperidol, 48.4 ± 3.89 cm/sec; DA manipulation: $p = .923$, FP duration: $p = .584$, FP variability: $p = .716$). Reaching movements differed between FP durations ($F(1, 16) = 5.029$, $p = .039$, $\eta_p^2 = 0.239$) in that they required, on average, more time to reach the target when the FP duration was long rather than short (Figure 5F; $t(16) = 2.24$, $p = .039$, $d_z = 0.54$). However, statistical analysis failed to detect any significant impact of DA blockade on movement times (mean \pm SEM: placebo, 469.8 ± 34 msec; sulpiride, 469.84 ± 4.06 msec; haloperidol, 504.2 ± 24.96 msec; $p = .336$).

Therefore, we found no evidence for extrapyramidal effects induced by our pharmacological manipulation. This result is not surprising in consideration of the relatively low dosage adopted for the DA antagonists combined with the relative young age of our participants. More broadly, this set of results indicates that the kinematics of the

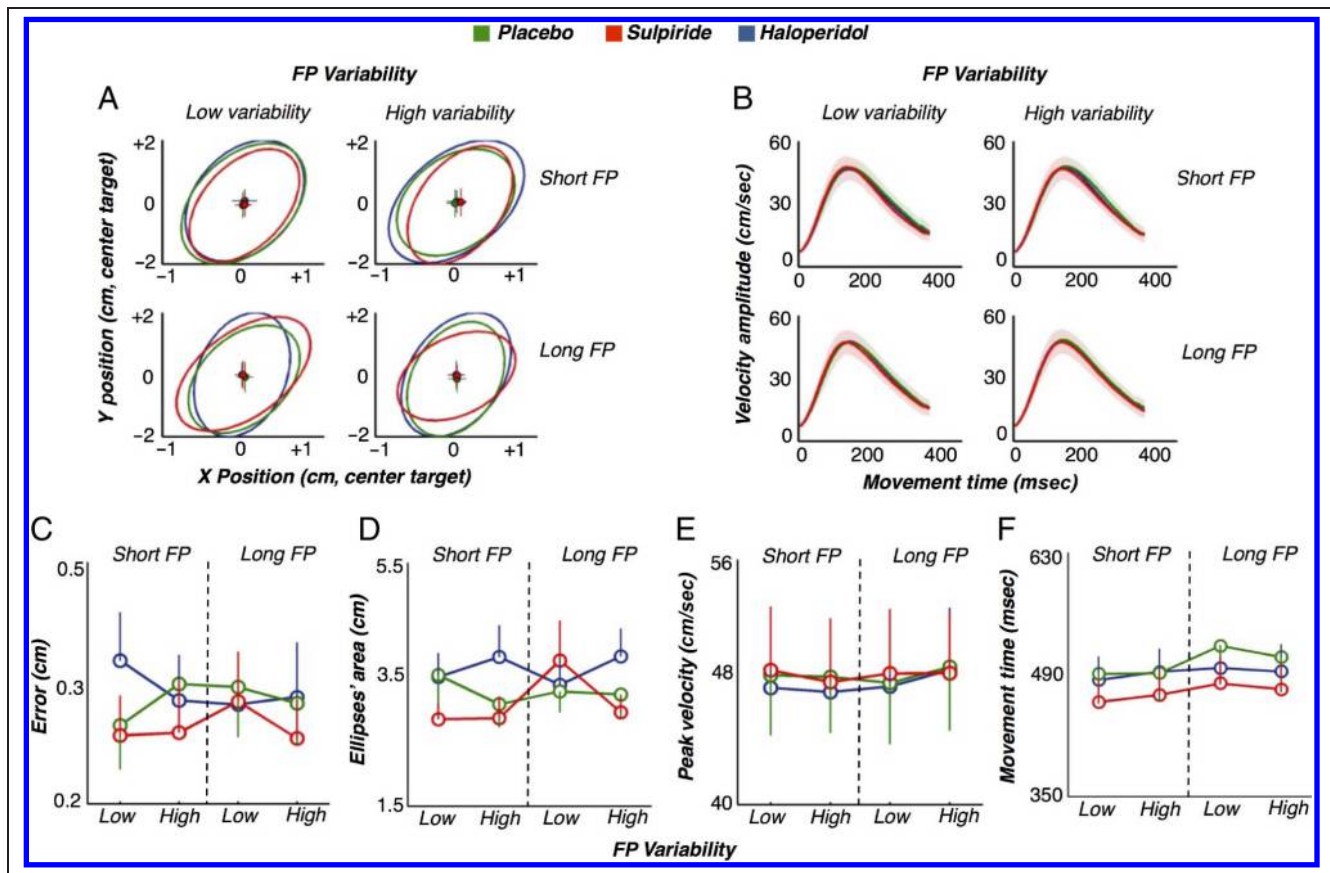


Figure 5. Kinematics of reaching movements. (A) Confidence ellipses encompassing 95% of reaching end-point population averaged across participants are shown for each level of FP variability (columns) and FP duration (rows). The colored points indicate the location of the ellipses' centroids with SEM in the horizontal and vertical coordinates. (B) Movement velocity profiles averaged across participants. Format follows the conventions established in A. (C and D) Mean reaching accuracy and precision measured as the distance of ellipse's centroid from target's center and ellipses' area, respectively. Neither reaching accuracy nor precision was systematically affected by our drug manipulations. (E and F) Movement velocity profiles (averaged across participants) and mean movement times were not significantly influenced by experimental manipulations. Error bars and shaded areas represent ± 1 SEM.

movements were similar irrespective of DA intervention or levels of actual or subjective temporal uncertainty.

DISCUSSION

This study provides novel evidence that DA blockade in humans impairs temporal preparation, that is, the temporal precision with which movement preparation is deployed. Specifically, we administered DA antagonists haloperidol and sulpiride in a double-blind placebo-controlled experiment to test for the role of DA in regulating temporal precision, a crucial requirement for temporal preparation of responses to forthcoming events (Piras & Coull, 2011). A variable FP paradigm was adapted to a reaching task to investigate temporal preparation under different levels of external and internal temporal uncertainties. The rationale for this approach is based on the idea that the brain needs to deal with internal and external sources of temporal uncertainty to allow for precise temporal preparation. Temporal preparation should be least precise when levels of temporal uncertainty are highest. We reasoned that, if DA influences subjective temporal uncertainty through its control of temporal precision, this effect should be further amplified under DA blockade. In our specific case, reduced temporal precision after DA blockade would be reflected by a stronger impact of internal and external uncertainties on temporal preparation.

We applied two different DA drugs because of their different affinity to D1 and D2 receptor families. Whereas sulpiride selectively blocks DA receptors of the D2 receptor family (O'Connor & Brown, 1982), haloperidol blocks both D1 and D2 receptor families (Zhang & Bymaster, 1999). Pharmacological studies in rats indicate that different DA receptor families might mediate distinct aspects of temporal preparation. D2 signaling, particularly in the striatum, is implicated in forming temporal expectations about stimulus occurrence across trials (Meck, 2006). Mesocortical D1 signaling, by contrast, is required to update temporal representations that encode the elapsed time within a trial (Parker et al., 2013). Thus, a differential effect of haloperidol and sulpiride on temporal preparation would provide indication for the possible roles of D1/D2 receptor activity in regulating temporal precision. Because forming temporal expectations across trials and temporal representations within trials can be mapped onto the marginal and conditional components of the subjective hazard function, we tested for selective effects of DA treatments on the level of subjective temporal uncertainty of such components as estimated by their Weber fractions.

DA Blockade Impairs Temporal Expectations and Representations

Under placebo, mean RS decreased when the IS onset was less predictable, both in conditions of high internal and external temporal uncertainties. This indicates that high temporal uncertainty reduces temporal preparation in an-

icipation of an event. Previous work has reported a general slowing of RS under DA blockade (Rammsayer, 1997). Here, we found that the ability for temporal preparation was impaired under haloperidol (Figure 2A). This was not because of a general increase in behavioral variability but of an effect on both temporal expectations (because of large biases) and temporal representations (because of low temporal sensitivity; Figure 2D). In particular, the decline in temporal expectation was observed only when temporal uncertainty was highest (Figure 2A). DA blockade produced a general flattening of slopes of the FP effects (Figure 2D). This indicates that, under DA blockade, temporal preparation can no longer rely on accurate temporal representations about the passage of time. This effect was significant for sulpiride only in conditions of high internal and external uncertainties, whereas haloperidol led to a significant decline in temporal sensitivity for high internal uncertainty regardless of external uncertainty.

This decline can be seen as an indication that conditions of high temporal uncertainty require more temporal precision than the participants can afford under DA blockade. Moreover, a three-way interaction suggested a progressive reduction of temporal sensitivity between the drugs, such that, under haloperidol, performance started declining at lower levels of external and internal temporal uncertainties, compared with sulpiride.

DA Blockade Impairs Temporal Preparation by Increasing Subjective Temporal Uncertainty

The model comparison revealed that subjective hazard functions with marginal and conditional components characterized by independent Weber fractions best accounted for the observed data (Figure 4A). This result seems to confirm that temporal preparation might be based on two separate mechanisms: one extracting the probability of stimulus occurrence across trials and the other updating such probability with the passage of time within a trial. The estimates from the fitted subjective hazard function revealed that the decline in temporal precision was accompanied by increased levels of subjective temporal uncertainty, as reflected by large estimated Weber fractions (Figure 4B–D). However, different DA treatments did not have significantly different effects on the Weber fractions of the marginal and conditional components. Therefore, our fitting confirms that the effects of DA blockade stemmed from overall increased levels of subjective temporal uncertainty.

The similar increase in subjective temporal uncertainty in both the marginal and conditional components of the model might appear at odds with the fact that our model comparison pointed to an advantage in treating the two components as independent. However, the advantage of treating the two model components separately appears clearly after the inspection of their Weber fractions under placebo, with the conditional component being less precise than its marginal counterpart (Figure 4B). In other words,

our estimates would suggest that the selected model has more explanatory power than the other models in the comparison set because it can account for such difference.

Systems Mediating Temporal Preparation and Reaching Movements Are Pharmacologically Dissociable

Conversely, neither temporal uncertainty nor DA blockade affected the precision and accuracy of reaching movements (Figure 5). This observation is in agreement with previous evidence showing that temporal uncertainty does not affect the precision of reaching movements (Georgopoulos, Kalaska, & Massey, 1981). This observation points to a dissociation between processes underlying reaching movements and those serving temporal preparation.

General Discussion

Previous work has also demonstrated differential effects of haloperidol and sulpiride on temporal precision (Rammsayer, 1997) or action reprogramming (Bestmann, Ruge, Rothwell, & Galea, 2015). Whereas atypical neuroleptics such as sulpiride primarily antagonize D2 receptors in the mesolimbic and mesocortical areas of the brain (Brücke et al., 1992), typical neuroleptics such as haloperidol have more widespread effects on D2 receptors. Therefore, it has been suggested (Meck, 1996; Rammsayer, 1993) that the deteriorating effect of haloperidol depends on its potency to block D2 receptors in the BG. This idea sides with the central role attributed to BG in interval timing (Coull et al., 2011; Matell & Meck, 2004).

Manipulations of nigrostriatal projections influence fixed-interval timing performance (Buhusi & Meck, 2005). Moreover, substantia nigra pars compacta and ventral tegmental area (VTA) DA neurons are sensitive to the expected time of reward (Waelti, Dickinson, & Schultz, 2001; Hollerman & Schultz, 1998; Schultz, Dayan & Montague, 1997), and their temporal precision declines with interval duration mimicking the decay of behavioral temporal precision (Fiorillo, Newsome, & Schultz, 2008). A central aspect of our results is that the impact of DA blockade on temporal preparation scaled with the level of external and internal temporal uncertainties. Because temporal precision is likely to be limited by internal and external sources of uncertainty, DA blockade could have compromised the ability to correctly keep track of time by deregulating the levels of subjective temporal uncertainty (Frank, 2005). As a consequence, temporal accuracy in estimating the mean FP would also be corrupted.

However, the BG have no exclusive role in temporal preparation; instead, they are part of a fronto-striatal loop critical to temporal preparation (Dale et al., 2010; Vallesi, McIntosh, Shallice, & Stuss, 2009; Matell & Meck, 2004). Compelling evidence on the involvement of prefrontal areas on keeping track of the passage of time comes from human neuroimaging (Vallesi et al., 2009) and TMS stud-

ies as well as animal neurophysiology. Indeed, reversible perturbation of human pFC with TMS can abolish the FP effect (Vallesi, Shallice, & Walsh, 2007).

Similarly, prefrontal D1 depletion in rodents produced weak FP effect, thus confirming the role of frontal DA circuits in forming temporal representations (Parker et al., 2013). This set of evidence supports the idea advanced by (Narayanan, Land, Solder, Deisseroth, & Dileone, 2012) that temporal preparation might rely on the orchestrated activity of VTA neurons encoding the timing of rewards (Fiorillo et al., 2008) and rodent prefrontal populations that encode the passage of time (Narayanan & Laubach, 2006). These authors showed that optogenetic manipulations of D1 signaling in VTA projections to the pFC specifically influenced fixed-interval timing performance. They further supported this view by noting that their manipulation did not influence kinematic parameters, consistent with previous work that investigated these projections on motor control (Narayanan et al., 2012).

In this study, we have observed a significant weakening of the FP effect only under haloperidol. Given the differential affinity between haloperidol (D2/D1) and sulpiride (D2), one could speculate that the inverted FP effect reported in this study could have arisen by the additional capacity of haloperidol to block prefrontal D1 receptors. This would also be supported by the lack of effects exerted by our manipulations on kinematic parameters of our motor task, consistent with Narayanan's results. However, this explanation needs to be qualified with the observation that the effect of sulpiride was not significant but nevertheless qualitatively similar to the haloperidol-mediated effect. This difference might be produced by virtue of the fact that haloperidol has greater receptor availability than sulpiride simply by acting on more than one receptor type. Furthermore, functional pathways mediated by D1 and D2 receptors, although possibly segregated, are not necessarily independent (Calabresi, Picconi, Tozzi, Ghiglieri, & Di Filippo, 2014). The weak effect of sulpiride on interval timing has been previously linked to its affinity mainly with D2 receptors in the mesolimbic DA system, whereas haloperidol also blocks D2 receptors in the nigrostriatal system (Coull et al., 2011). Hence, one possible account for our results is that haloperidol's action on the nigrostriatal system might have decreased the precision (and thus increased the uncertainty) of interval timing, upon which the formation of both temporal expectations and temporal representations relies. Similar levels of subjective temporal uncertainty introduced by haloperidol on temporal expectations and representations (estimated by fitting subjective hazard functions) corroborate this view.

Previously, the subjective hazard function has been successfully employed to describe temporal preparation (Tsunoda & Kakei, 2011; Bueti et al., 2010; Janssen & Shadlen, 2005). However, here, we propose that a canonical implementation of the subjective hazard function, in which $f(t)$ (representing the component forming temporal expectation across trials) and $F(t)$ representing the component updating the expectation within a trial) share the

same Weber fraction, would fail to capture the relative contributions of the processes underpinning temporal preparation in variable timing tasks. On the contrary, when $f(t)$ and $F(t)$ are treated as two separate components of the same model, temporal preparation can be separated into two components: one reflecting the temporal precision (or uncertainty) of mechanisms that form temporal expectations between trials and another forming temporal representations within trials. This creates a conceptual bridge between the mechanisms at the base of learning temporal context and tracking the passage of time and, on the other hand, a broad measure of temporal preparation such as RTs.

The combination of pharmacological interventions together with a model-based approach allows for the dissection of different processes involved in various forms of timing and could provide a fruitful way to identify specific mechanisms impaired in clinical conditions characterized by altered timing. For example, because flattened FP effects have been described in a subpopulation of Parkinsonian patients (Jurkowski, Stepp, & Hackley, 2005; Bloxham et al., 1987), characterized by pronounced frontal damage (Coull et al., 2011), the prediction for our model would be a stronger reduction in temporal precision in the component responsible for the updating of temporal representations.

In conclusion, we show for the first time that DA antagonist haloperidol impairs the ability to prepare movements based on estimates about the most likely time of occurrence of events. This impairment stems from the inability to infer temporal structure from events across trials together with the compromised capacity to keep track of the passage of time within a trial, which prevents the formation of precise temporal preparation. The detrimental effect of DA blockade on temporal preparation increases with the level of both external and internal temporal uncertainties and is accompanied with high levels of subjective temporal uncertainty. This suggests that, under DA blockade, the precision with which we process time is inadequate to deal with high levels of temporal uncertainty. Furthermore, it provides novel direct evidence that DA regulates the precision with which we process time when preparing for an action.

Acknowledgments

This work was funded by the European Research Council project ActSelectContext (260424). Diane Ruge was funded by the Tourette Syndrome Association, USA, and the Dorothy Feiss Research Grant.

Reprint requests should be sent to Alessandro Tomassini, Sobell Department of Motor Neuroscience and Movement Disorders, UCL Institute of Neurology, University College London, 33 Queen Square, London WC1N 3BG, United Kingdom, or via e-mail: a.tomassini@ucl.ac.uk.

REFERENCES

- Artieda, J., Pastor, M. A., Lacruz, F., & Obeso, J. A. (1992). Temporal discrimination is abnormal in Parkinson's disease. *Brain*, *115*, 199–210.
- Barlow, H. B. (1964). Dark-adaptation: A new hypothesis. *Vision Research*, *4*, 47–58.
- Beck, J. M., Ma, W. J., Pitkow, X., Latham, P. E., & Pouget, A. (2012). Not noisy, just wrong: The role of suboptimal inference in behavioral variability. *Neuron*, *74*, 30–39.
- Bertelson, P., & Tisseyre, F. (1969). The time-course of preparation: Confirmatory results with visual and auditory warning signals. *Acta Psychologica*, *120*, 199–226.
- Bestmann, S., Ruge, D., Rothwell, J., & Galea, J. M. (2015). The role of dopamine in motor flexibility. *Journal of Cognitive Neurosciences*, *27*, 365–376.
- Brücke, T., Roth, J., Podreka, I., Strobl, R., Wenger, S., & Asenbaum, S. (1992). Striatal dopamine D2-receptor blockade by typical and atypical neuroleptics. *Lancet*, *339*, 497.
- Bueti, D., Bahrami, B., Walsh, V., & Rees, G. (2010). Encoding of temporal probabilities in the human brain. *Journal of Neuroscience*, *30*, 4343–4352.
- Buhusi, C. V., & Oprisan, S. A. (2013). Time-scale invariance as an emergent property in a perceptron with realistic, noisy neurons. *Behavioral Processes*, *95*, 60–70.
- Buhusi, C. V., & Meck, W. H. (2005). What makes us tick? Functional and neural mechanisms of interval timing. *Nature Reviews Neuroscience*, *6*, 755–765.
- Burton, C. L., Strauss, E., Hultsch, D. F., Moll, A., & Hunter, M. (2006). Intraindividual variability as a marker of neurological dysfunction: A comparison of Alzheimer's disease and Parkinson's disease. *Journal of Clinical and Experimental Neuropsychology*, *28*, 67–83.
- Calabresi, P., Picconi, B., Tozzi, A., Ghiglieri, V., Di Filippo, M. (2014). Direct and indirect pathways of basal ganglia: A critical reappraisal. *Nature Neuroscience*, *17*, 1022–1030.
- Cohen, J. (1988). *Statistical power analysis for the behavioral sciences*. Mahwah, NJ: Erlbaum.
- Coull, J. T., Cheng, R. K., & Meck, W. H. (2011). Neuroanatomical and neurochemical substrates of timing. *Neuropsychopharmacology*, *36*, 3–25.
- Coull, J. T., & Nobre, A. C. (1998). Where and when to pay attention: The neural systems for directing attention to spatial locations and to time intervals as revealed by both PET and fMRI. *Journal of Neuroscience*, *18*, 7426–7435.
- Dale, C. L., Findlay, A. M., Adcock, R. A., Vertinski, M., Fisher, M., Genevsky, A., et al. (2010). Timing is everything: Neural response dynamics during syllable processing and its relation to higher-order cognition in schizophrenia and healthy comparison subjects. *International Journal of Psychophysiology*, *75*, 183–193.
- Deleu, D., Northway, M. G., & Hanssens, Y. (2002). Clinical pharmacokinetic and pharmacodynamic properties of drugs used in the treatment of Parkinson's disease. *Clinical Pharmacokinetics*, *41*, 261–309.
- Drazin, D. H. (1961). Effects of foreperiod, foreperiod variability, and probability of stimulus occurrence on simple reaction time. *Journal of Experimental Psychology*, *62*, 43–50.
- Fiorillo, C. D., Newsome, W. T., & Schultz, W. (2008). The temporal precision of reward prediction in dopamine neurons. *Nature Neuroscience*, *11*, 966–973.
- Frank, M. J. (2005). Dynamic dopamine modulation in the basal ganglia: A neurocomputational account of cognitive deficits in medicated and nonmedicated Parkinsonism. *Journal of Cognitive Neuroscience*, *17*, 51–72.
- Frank, M. J., & O'Reilly, R. C. (2006). A mechanistic account of striatal dopamine function in human cognition: Psychopharmacological studies with cabergoline and haloperidol. *Behavioral Neuroscience*, *120*, 497–517.
- Friston, K. J., Shiner, T., FitzGerald, T., Galea, J. M., Adams, R., Brown, H., et al. (2012). Dopamine, affordance and active inference. *PLoS Computational Biology*, *8*, e1002327.

- Galea, J. M., Bestmann, S., Beigi, M., Jahanshahi, M., & Rothwell, J. C. (2012). Action reprogramming in Parkinson's disease: Response to prediction error is modulated by levels of dopamine. *Journal of Neuroscience*, *32*, 542–550.
- Georgopoulos, P., Kalaska, J. F., & Massey, J. T. (1981). Spatial trajectories and reaction times of aimed movements: Effects of practice, uncertainty, and change in target location. *Journal of Neurophysiology*, *46*, 725–743.
- Gibbon, J. (1977). Scalar expectancy theory and Weber's law in animal timing. *Psychological Review*, *84*, 279–325.
- Goldstone, S. (1968). Reaction time to onset and termination of lights and sounds. *Perceptual and Motor Skills*, *27*, 1023–1029.
- Hackley, S. A., Langner, R., Rolke, B., Erb, M., Grodd, W., & Ulrich, R. (2009). Separation of phasic arousal and expectancy effects in a speeded reaction time task via fMRI. *Psychophysiology*, *46*, 163–171.
- Hollerman, J. R., & Schultz, W. (1998). Dopamine neurons report an error in the temporal prediction of reward during learning. *Nature Neuroscience*, *1*, 304–309.
- Janssen, P., & Shadlen, M. N. (2005). A representation of the hazard rate of elapsed time in macaque area LIP. *Nature Neuroscience*, *8*, 234–241.
- Jurkowski, A. J., Stepp, E., & Hackley, S. A. (2005). Variable foreperiod in Parkinson's disease: Dissociation across reflexive and behaviors. *Brain and Cognition*, *58*, 49–61.
- Karlin, L. (1959). Reaction time as a function of foreperiod duration and variability. *Journal of Experimental Psychology*, *58*, 185–191.
- Klemmer, E. T. (1956). Time uncertainty in simple reaction time. *Journal of Experimental Psychology*, *51*, 179–184.
- Korchounov, A., & Ziemann, U. (2011). Neuromodulatory neurotransmitters influence LTP-like plasticity in human cortex: A pharmac-TMS study. *Neuropsychopharmacology*, *36*, 1894–1902.
- Lake, J. I., & Meck, W. H. (2013). Differential effects of amphetamine and haloperidol on temporal reproduction: Dopaminergic regulation of attention and clock speed. *Neuropsychologia*, *51*, 284–292.
- Lustig, C., & Meck, W. H. (2005). Chronic treatment with haloperidol induces deficits in working memory and feedback effects of interval timing. *Brain and Cognition*, *58*, 9–16.
- Matell, M. S., & Meck, W. H. (2004). Cortico-striatal circuits and interval timing: Coincidence detection of oscillatory processes. *Brain Research, Cognitive Brain Research*, *21*, 139–170.
- Meck, W. H. (1996). Neuropharmacology of timing and time perception. *Cognitive Brain Research*, *3*, 227–242.
- Meck, W. H. (2006). Neuroanatomical localization of an internal clock: A functional link between mesolimbic, nigrostriatal, and mesocortical dopaminergic systems. *Brain Research*, *1109*, 93–107.
- Narayanan, N. S., Land, B. B., Solder, J. E., Deisseroth, K., & Dileone, R. J. (2012). Prefrontal D1 dopamine signaling is required for temporal control. *Proceedings of the National Academy of Sciences*, *109*, 20726–20731.
- Narayanan, N. S., & Laubach, M. (2006). Top-down control of motor cortex ensembles by dorsomedial prefrontal cortex. *Neuron*, *52*, 921–931.
- Niemi, P., & Näätänen, R. (1981). Foreperiod and simple reaction time. *Psychological Bulletin*, *89*, 133–162.
- O'Connor, S. E., & Brown, R. A. (1982). The pharmacology of Sulpiride—A dopamine receptor antagonist. *General Pharmacology*, *13*, 185–193.
- Parker, K. L., Alberico, S. L., Miller, A. D., & Narayanan, N. S. (2013). Prefrontal D1 dopamine signaling is necessary for temporal expectation during reaction time performance. *Neuroscience*, *255*, 246–254.
- Piras, F., & Coull, J. T. (2011). Implicit, predictive timing draws upon the same scalar representation of time as explicit timing. *PLoS One*, *6*, e18203.
- Praamstra, P., & Pope, P. (2007). Slow brain potential and oscillatory EEG manifestations of impaired temporal preparation in Parkinson's disease. *Journal of Neurophysiology*, *98*, 2848–2857.
- Rammsayer, T. (1989). Is there a common dopaminergic basis of time perception and reaction time? *Neuropsychobiology*, *21*, 37–42.
- Rammsayer, T. H. (1993). On dopaminergic modulation of temporal information processing. *Biological Psychology*, *36*, 209–222.
- Rammsayer, T. H. (1997). Are there dissociable roles of the mesostriatal and mesolimbocortical dopamine systems on temporal information processing in humans? *Neuropsychobiology*, *35*, 36–45.
- Ratcliff, R. (1993). Methods for dealing with reaction time outliers. *Psychological Bulletin*, *114*, 510–532.
- Reed, C. L., & Franks, I. M. (1998). Evidence for movement preprogramming and on line control in differentially impaired patients with Parkinson's disease. *Cognitive Neuropsychology*, *15*, 723–745.
- Revol, P., Rossetti, Y., Vighetto, A., Rode, G., Boisson, D., & Pisella, L. (2003). Pointing errors in immediate and delayed conditions in unilateral optic ataxia. *Spatial Vision*, *16*, 347–364.
- Rigoux, L., Stephan, K. E., Friston, K. J., & Daunizeau, J. (2014). Bayesian model selection for group studies—Revisited. *Neuroimage*, *84*, 971–985.
- Rolls, E. T., Thorpe, S. J., Boytim, M., Szabo, I., & Perrett, D. I. (1984). Responses of striatal neurons in the behaving monkey. 3. Effects of iontophoretically applied dopamine on normal responsiveness. *Neuroscience*, *12*, 1201–1212.
- Schultz, W., Dayan, P., & Montague, P. R. (1997). A neural substrate of prediction and reward. *Science*, *275*, 1593–1599.
- Smith, J. G., Harper, D. N., Gittings, D., & Abernethy, D. (2007). The effect of Parkinson's disease on time estimation as a function of stimulus duration range and modality. *Brain and Cognition*, *64*, 130–143.
- Stephan, K. E., Penny, W. D., Daunizeau, J., Moran, J. R., & Friston, K. J. (2009). Bayesian model selection for group studies. *Neuroimage*, *46*, 1004–1017.
- Tomasi, D., Wang, G. J., Studentsova, Y., & Volkow, D. (2014). Dissecting neural responses to temporal prediction, attention and memory: Effects of reward learning and interoception on time perception. *Cerebral Cortex*, *25*, 1–12.
- Tsunoda, Y., & Kakei, S. (2011). Anticipation of future events improves the ability to estimate elapsed time. *Experimental Brain Research*, *214*, 323–334.
- Vallesi, A., McIntosh, A. R., Shallice, T., & Stuss, D. T. (2009). When time shapes behavior: fMRI evidence of brain correlates of temporal monitoring. *Journal of Cognitive Neuroscience*, *21*, 1116–1126.
- Vallesi, A., Shallice, T., & Walsh, V. (2007). Role of the prefrontal cortex in the foreperiod effect: TMS evidence for dual mechanisms in temporal preparation. *Cerebral Cortex*, *17*, 466–474.
- Waelti, P., Dickinson, A., & Schultz, W. (2001). Dopamine responses comply with assumptions of formal learning theory. *Nature*, *412*, 43–48.
- Zhang, W., & Bymaster, F. P. (1999). The in vivo effects of olanzapine and other antipsychotic agents on receptor occupancy and antagonism of dopamine D1, D2, D3, 5HT 2A and muscarinic receptors. *Psychopharmacology*, *141*, 267–278.